Design of High-Resolution Cosine-Modulated Transmultiplexers with Sharp Transition Band

Paulo S. R. Diniz, *Fellow, IEEE*, Luiz C. R. de Barcellos, and Sergio L. Netto, *Member, IEEE*

***Abstract*—Due to the growing importance of multichannel modulation, there has been great interest in the design of high-performance transmultiplex systems. In this paper, a new cosine-modulated transmultiplex structure is proposed based on a prototype filter designed with the frequency-response masking (FRM) approach. This new structure leads to substantial reduction in the computational complexity (number of multiplications per output sample) of the prototype filters having sharp transition band and equivalently small roll-off values. The relation between the interpolation factor used in the FRM prototype filter and the decimation factor in the subbands leads to distinct structures. Examples included indicate that the reduction in computational complexity can be higher than 50% of the current state-of-art designs, whereas the reduction on the number of distinct coefficients of the prototype filter can be reduced even further (over 75%). As a result, the proposed approach allows the design of very selective subfilters for transmultiplexes with a very large number of subchannels.**

***Index Terms*—Cosine-modulated filterbanks, cosine-modulated transmultiplexers, extended lapped transforms, filterbanks, frequency response masking, high-resolution spectral analysis, multirate systems, sharp transition band filters, transmultiplexers.**

I. Introduction

MULTICHANNEL modulation methods play a key role in modern data transmission channels with severe and moderate intersymbol interference (ISI). The key idea behind the success of this technique is the partition of a physical channel in nonoverlapping narrowband subchannels through a transmultiplexer. If the subchannels are narrow enough, the associated channel response in each subchannel frequency range appears to be flat, avoiding the use of equalizers. In addition, the subchannel division allows, whenever possible, the exploitation of signal-to-noise ratio (SNR) in the different subbands in order to manage the dataload in each subchannel. Typically, subchannels with high SNR utilize high-order modulation, whereas subchannels with moderate SNR lower order modulation should be used. On the other hand, subchannels with severe interference are not used for data transmission. Such schemes are employed in a number of high-speed digital subscriber line (xDSL) systems.

Manuscript received October 9, 2002; revised June 12, 2003. The associate editor coordinating the review of this manuscript and approving it for publication was Prof. Trac D. Tran.

P. S. R. Diniz and S. L. Netto are with the Programa de Engenharia Elétrica-COPPE/EE/UFRJ, Rio de Janeiro, RJ, 21945-970, Brazil (e-mail: diniz@lps.ufrj.br; sergioln@lps.ufrj.br).

L. C. R. de Barcellos was with the Programa de Engenharia Elétrica-COPPE/EE/UFRJ, Rio de Janeiro, RJ, 21945-970, Brazil. He is now with Petrobras, Rua Gerneral Canabarro 500, 11o andar, Rio de Janeiro, RJ, Brazil.

Digital Object Identifier 10.1109/TSP.2004.826157

A critical component of the multichannel systems is the filterbank-based transmultiplex (TMUX). The ideal situation requires the design of highly selective filterbanks to avoid crosstalk between subchannels and that the subfilter frequency responses are narrow enough such that channel response in each subband appears to be flat. The latter condition is achieved by filterbanks with a very large number of subbands, whose design with the currently available techniques leads to an optimization problem with a prohibitive number of parameters.

The cosine-modulated transmultiplex (CMT) is very popular in applications requiring a large number of subbands due to their easy design and efficient implementation, in terms of computational complexity [1]–[5]. However, with the current state of the art, one is not able to design CMTs meeting the demanding requirements of multichannel systems, including large number of channels (above 1000, for instance) with low levels of ISI and intercarrier interference (ICI).

A possible strategy is to employ the frequency-response masking (FRM) approach to design the prototype filter of the CMT. The FRM is an efficient method for designing linear-phase finite impulse response (FIR) digital filters with general passbands and sharp transition bands. With such a method, by allowing a small increase in the filter group delay, it is possible to reduce the overall filter complexity (number of arithmetic operations required per output sample) when compared with standard design methods. In fact, it has been verified that the FRM approach can achieve a reduction to about 30% of the number of coefficients required by a minimax FIR filter design realized in direct form [6], [7]. Recent results show that the FRM framework can be generalized to accommodate different structures and approximation methods [8]–[10]. Unfortunately, the application of FRM to design computationally efficient CMT is not straightforward and requires careful investigation.

In this paper, a solution to design CMTs with a reduced number of distinct parameters to be optimized is presented. The approach is feasible due to a judicious use of the FRM approach, as opposed to standard design methods, to design the CMT prototype filter. As an illustration, it is verified that with the FRM prototype filter, the parameters of interest of a TMUX system (namely, the attenuation, the overall delay, and the ISI and ICI levels) are comparable with those in the standard design, whereas the number of coefficients can be reduced substantially (down to about 50% of the original number). Therefore, it is possible to achieve complexity reduction in a CMT structure without sacrificing other design requirements.

The relation between the interpolation factor used in the CMT prototype filter and the FRM decimation factor in the subbands

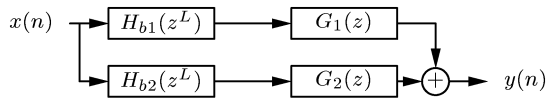

Fig. 1. Basic realization of an FIR filter using the FRM approach, depicting the positive (upper) and the negative (lower) branches of the FRM filter.

leads to different structures that all have a small number of distinct coefficients when compared with the standard structure. The reduction in the number of coefficients (to about 25% of the original number of distinct parameters) opens new venues for the possible design of filterbanks with sharp transition band and with a large number of subbands, as demonstrated in the design examples.

The organization of this paper is as follows: In Sections II and III, we briefly describe the main ideas behind the FRM approach and the CMT systems, respectively. In Section IV, we propose an efficient structure of CMT systems, and in Section V, design examples are included, illustrating the advantages of the proposed method. Through these examples, we illustrate how the proposed method is capable of designing multichannel communications systems with a very large number of channels, requiring a quite reduced number of distinct coefficients. Such a reduced number of distinct parameters allows a faster optimization procedure when figures of merit, such as ISI and ICI, are considered in the design process.

II. Frequency-Response Masking Approach

The basic block diagram for the FRM approach can be seen in Fig. 1. In this scheme, if we use an interpolation factor of L, the so-called interpolated base filter $H_{b1}(z^L)$ presents a repetitive frequency spectrum whose output signal is processed by the positive masking filter $G_1(z)$, of order N_m^+, in the upper branch of this realization. Similarly, a complementary version of this repetitive frequency response $H_{b2}(z^L)$ is in cascade with the negative masking filter $G_2(z)$, of order N_m^-, in the lower branch of the realization. In this procedure, both masking filters keep some of the spectrum repetitions within the desired passband, which are added together to compose the desired frequency response. These operations are depicted in Fig. 2, where one can clearly see the sharp transition band in the resulting response.

If the base filter has linear-phase and an even order N_b, its direct and complementary transfer functions, interpolated by a factor of L, are given by

$$H_{b1}(z^L) = \sum_{i=0}^{N_b} h_b(i) z^{-Li} \tag{1}$$

$$H_{b2}(z^L) = z^{-\frac{N_b}{2}} - \sum_{i=0}^{N_b} h_b(i) z^{-Li} \tag{2}$$

respectively, where $h_b(n)$ is the impulse response of the base filter.

The design specifications of each FRM subfilter can be found in the original paper [6]. The value of L that minimizes the overall number of multiplications can be obtained by estimating

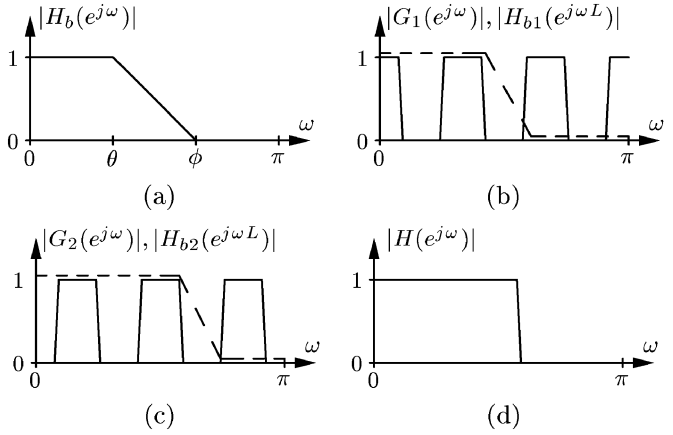

Fig. 2. Combination of the frequency responses in the upper and lower branches generating the FRM filter with very narrow transition band. (a) Base filter. (b) Positive masking operation. (c) Negative masking operation. (d) Resulting response.

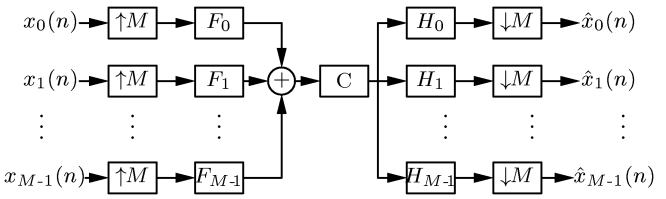

Fig. 3. Block diagram for an M-channel TMUX.

the lengths of all subfilters for various L and either finding the best case scenario heuristically or using the strategy detailed in [7]. Then, it is possible to optimize the responses of the subfilters by using a variety of algorithms [8]–[10]. If the transition band is not too sharp when compared with the passband, then it is possible to discard the lower branch of the FRM filter, further reducing the number of coefficients in the overall filter. In addition, the specifications of the subfilters can be relaxed, using the concept of "don't care bands" since there is no overlap between the frequency responses of the FRM upper and lower branches as described in [6].

III. TMUX Configuration

The TMUX is an application of filterbanks in which the signals coming from various sources are interpolated, filtered by a synthesis bank, and added together to compose a single signal for transmission over a given channel C [1], [5]. At the receiver, the analysis filters split the transmitted signal back into M channels, where each output corresponds to one original input source. If the TMUX has perfect reconstruction (PR), then the output signals are equal to the source signals when the channel model is a pure delay, whereas if the estimated signals receive small interference from the other sources, we have the nearly perfect reconstruction (NPR) case. Fig. 3 depicts the block diagram for such system.

The main advantage of using a CMT is the fact that only one prototype filter design is required [1], [11]–[13] since the synthesis and analysis filters are obtained by modulating this filter with a proper cosine function. For the prototype filter, the 3-dB

attenuation point and the stopband edge of the magnitude response are located at

$$\omega_{3\text{ dB}} \approx \frac{\pi}{(2M)}; \quad \omega_s = \frac{(1+\rho)\pi}{2M} \tag{3}$$

respectively, where ρ is the so-called roll-off factor.

If the prototype filter of order N_p has a transfer function

$$H_p(z) = \sum_{n=0}^{N_p} h_p(n) z^{-n} \tag{4}$$

then the impulse responses of the analysis and the synthesis filters are given, respectively, by

$$h_m(n) = 2h_p(n)\cos\left[\frac{(2m+1)\left(n-\frac{N_p}{2}\right)\pi}{2M} + (-1)^m\frac{\pi}{4}\right] \tag{5}$$

$$f_m(n) = 2h_p(n)\cos\left[\frac{(2m+1)\left(n-\frac{N_p}{2}\right)\pi}{2M} - (-1)^m\frac{\pi}{4}\right] \tag{6}$$

for $m = 0, 1, \ldots, (M-1)$, and $n = 0, 1, \ldots, N_p$.

If the prototype filter has $2KM$ coefficients, then it is possible to decompose it into $2M$ polyphase components

$$H_p(z) = \sum_{j=0}^{2M-1} z^{-j} E_j(z^{2M}) \tag{7}$$

where the polyphase components $E_j(z)$ are given by

$$E_j(z) = \sum_{k=0}^{K-1} h_p(2kM + j) z^{-k}. \tag{8}$$

Therefore, the analysis filter can be written as[1]

$$H_m(z) = \sum_{j=0}^{2M-1} c_{m,j} z^{-j} E_j(-z^{2M}) \tag{9}$$

where

$$c_{m,j} = 2\cos\left[\frac{(2m+1)\left(j-\frac{N_p}{2}\right)\pi}{2M} + (-1)^m\frac{\pi}{4}\right] \tag{10}$$

such that

$$c_{m,(j+2kM)} = (-1)^k c_{m,j}. \tag{11}$$

[1]The same procedure can be applied to the synthesis filters.

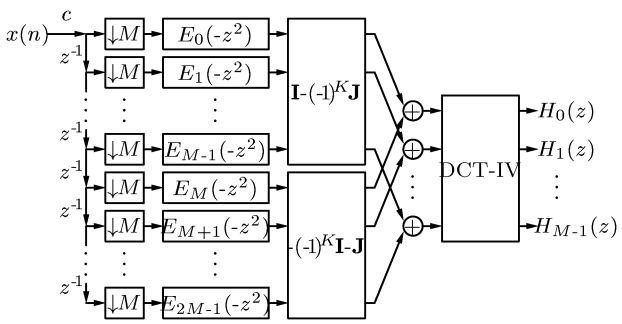

Fig. 4. Efficient CMT structure.

From (9), we can define a vector containing the transfer functions of the analysis filters as follows:

$$\begin{bmatrix} H_0(z) \\ H_1(z) \\ \vdots \\ H_{M-1}(z) \end{bmatrix} = [\mathbf{C_1} \quad \mathbf{C_2}] \begin{bmatrix} E_0(-z^{2M}) \\ z^{-1}E_1(-z^{2M}) \\ \vdots \\ z^{-(2M-1)}E_{2M-1}(-z^{2M}) \end{bmatrix}. \tag{12}$$

The two matrix $\mathbf{C_1}$ and $\mathbf{C_2}$ are related to the DCT-IV matrix as follows:

$$\mathbf{C}_1 = c\,\mathbf{C^{IV}}\left[\mathbf{I} - (-1)^K\mathbf{J}\right] \tag{13}$$

$$\mathbf{C}_2 = c\,\mathbf{C^{IV}}\left[-(-1)^K\mathbf{I} - \mathbf{J}\right] \tag{14}$$

where $c = \sqrt{M}(-1)^{\lfloor K/2 \rfloor}$, with $\lfloor x \rfloor$ representing the largest integer less than or equal to x, $\mathbf{I}$ is the identity matrix, and $\mathbf{J}$ is the reverse (flipped) identity matrix, and each element of the DCT-IV matrix is given by

$$[\mathbf{C^{IV}}]_{m,n} = \sqrt{\frac{2}{M}}\cos\left[\frac{2m+1}{2M}\left(n+\frac{1}{2}\right)\pi\right]. \tag{15}$$

The efficient structure for the CMT related to (12) is depicted in Fig. 4. From this figure, one infers that the CMT realization requires only (N_p+1) multiplications for the polyphase components, one multiplication by c, the premodulating matrices consisting of $[\mathbf{I} - (-1)^K\mathbf{J}]$, $[-(-1)^K\mathbf{I} - \mathbf{J}]$, and the DCT-IV. The overall number of multiplications per output sample (not taking into consideration any symmetry of coefficients) is then

$$\mathcal{C} = K + \alpha \tag{16}$$

where α is associated with the multiplication by the constant c and the modulating matrices, which can be implemented using fast algorithms [14]. The polyphase decomposition turns the value of $\mathcal{C}$ small, independent of the number of channels M, demonstrating the efficiency of the structure.

If the prototype filter has symmetric impulse response, then it is possible to use the butterfly-based structures proposed by Malvar [2], [11], depicted in Fig. 5. The resulting filterbank has perfect reconstruction. If it is desired to design an NPR filterbank, a modified structure can be used instead [3], [5]. In the

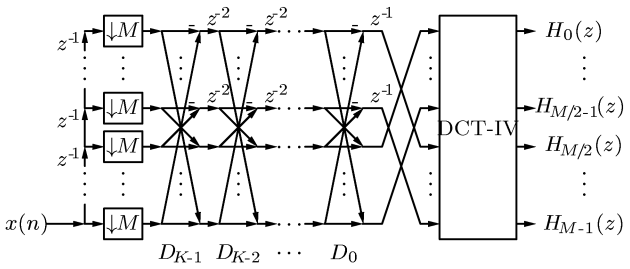

Fig. 5. Improved CMT structure using butterflies for the PR case.

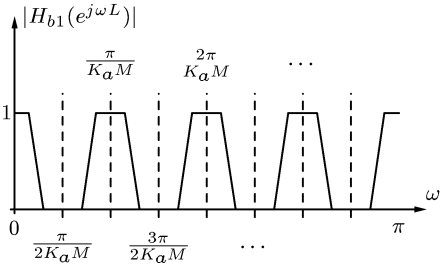

Fig. 6. For $L = 2K_aM$, the passbands of the interpolated base filter are centered on $(2k\pi)/(L)$, which include $(\pi)/(2M)$, where the $\omega_{3\text{ dB}}$ frequency for the CMT prototype filter should be.

case of Fig. 5, the D_k stages of butterflies can be viewed as matrices with nonzero elements only at the main diagonals, thus reducing the computational complexity to about 25% of the value obtained with the polyphase decomposition.

The transfer matrix, which includes all transfer functions from input a to output b, for the TMUX case has the following elements:

$$\left[\mathbf{T}(z^M)\right]_{a,b} = \sum_{k=0}^{M-1} H_a\left(ze^{\frac{-j2\pi k}{M}}\right) F_b\left(ze^{\frac{-j2\pi k}{M}}\right). \quad (17)$$

The ISI and ICI can be estimated with the following expressions [5]:

$$\text{ISI} = \max_k \left\{ \sum_n \left[\delta(n) - t_k(n)\right]^2 \right\} \quad (18)$$

$$\text{ICI} = \max_{k,\omega} \left\{ \sum_{l=0,k\neq l}^{M-1} \left| \left[\mathbf{T}(e^{j\omega})\right]_{k,l} \right|^2 \right\} \quad (19)$$

where $\delta(n)$ is the ideal impulse, $t_k(n)$ is the impulse response for the kth channel output, and the term $[\mathbf{T}(e^{j\omega})]_{k,l}$ is the crosstalk between the kth and lth channels, which can be determined from (17).

IV. FRM Design for the Prototype Filter

Let us first consider only the upper branch of the FRM structure in Fig. 1 as the prototype filter for the CMT. Then, the transfer functions for the analysis filters become

$$H_m(z) = \sum_{n=0}^{N} c_{m,n} \left(h_{b1}^I * g_1\right)(n) z^{-n} \quad (20)$$

where the term $(h_{b1}^I * g_1)(n)$ denotes the convolution between the interpolated base filter and the positive masking filter responses, and N is the overall order of the FRM filter. The key point is to find an efficient structure to calculate the convolution in (20), which takes into consideration the special property of the cosine functions for each sample. Assuming that $H_{b1}(z)$ and $G_1(z)$ have orders N_b and N_m^+, respectively, and using the definition of convolution, (20) can be rewritten as

$$H_m(z) = \sum_{i=0}^{N_b} \left[h_b(i) z^{-Li} \sum_{n=0}^{N_m^+} c_{m,(n+Li)} g_1(n) z^{-n} \right]. \quad (21)$$

The key problem is to find the proper values for L such that this convolution allows us to exploit the relationship of (11).

A. Solution for L Multiple of $2M$

We start by noting that if the interpolated filter has interpolation factor of $L = 2K_aM$, with K_a being an integer greater than zero, then (21) becomes

$$H_m(z) = \sum_{i=0}^{N_b} \left[h_b(i) z^{-Li} \sum_{n=0}^{N_m^+} c_{m,(n+2K_aMi)} g_1(n) z^{-n} \right] \quad (22)$$

and using the cosine relationship in (11), we have

$$\begin{aligned} H_m(z) &= \sum_{i=0}^{N_b} \left[h_b(i) z^{-Li} \sum_{n=0}^{N_m^+} (-1)^{K_a i} c_{m,n} g_1(n) z^{-n} \right] \\ &= \left[\sum_{i=0}^{N_b} (-1)^{K_a i} h_b(i) z^{-Li} \right] \left[\sum_{n=0}^{N_m^+} c_{m,n} g_1(n) z^{-n} \right] \end{aligned} \quad (23)$$

Therefore, it is possible to resolve the convolution problem by using a cascade of two filters. The masking filter can be decomposed by using polyphase decomposition. Unfortunately, for the cases in which $L = 2K_aM$, it is not possible to compose a prototype filter using the FRM approach since the desirable transition band of the prototype filter is not realizable. This occurs because the center frequency of one of the bands of the interpolated filter (or its complementary version) traverses the frequency $\omega_{3\text{ dB}}$ of the transition band of the CMT prototype filter, as depicted in Fig. 6. Therefore, it is not possible to satisfy the condition of (3).

B. Solution for M Multiple of L

Nevertheless, it is possible to find an efficient implementation for (21) in the cases where $L = M/K_b$, with K_b being an integer greater than zero, since in those cases, the transition band is realizable. In this case, (21) becomes

$$H_m(z) = \sum_{i=0}^{N_b} \left[h_b(i) z^{-Li} \sum_{n=0}^{N_m^+} c_{m,\left(n+\frac{M}{K_b}i\right)} g_1(n) z^{-n} \right]. \quad (24)$$

The idea is now to decompose not only the masking filter but the base filter as well, in order to solve (24). By decomposing first the interpolated base filter into $Q = 2K_b$ polyphase components

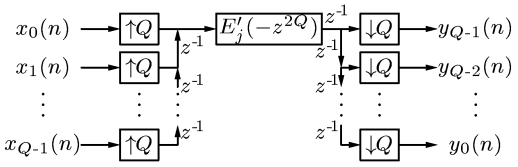

Fig. 7. Multiple-signal filtering structure.

and assuming that the base filter has QK_c coefficients, where K_c is a positive integer, we can write

$$\begin{aligned} H_m(z) &= \sum_{q=0}^{Q-1}\sum_{k=0}^{K_c-1}\Bigg[h_b(kQ+q)z^{-L(kQ+q)} \\ &\qquad \times \sum_{n=0}^{N_m^+} c_{m,\left[n+\frac{M}{K_b}(kQ+q)\right]}\, g_1(n)z^{-n}\Bigg] \\ &= \sum_{q=0}^{Q-1}\sum_{k=0}^{K_c-1}\Bigg[h_b(kQ+q)z^{-L(kQ+q)} \\ &\qquad \times \sum_{n=0}^{N_m^+} c_{m,\left[n+\left(2kM+\frac{M}{K_b}q\right)\right]}\, g_1(n)z^{-n}\Bigg]. \end{aligned} \tag{25}$$

Then, by using the cosine relationship of (11), we obtain

$$\begin{aligned} H_m(z) = \sum_{q=0}^{Q-1}\sum_{k=0}^{K_c-1}\Bigg[&h_b(kQ+q)(-1)^k z^{-L(kQ+q)} \\ &\times \sum_{n=0}^{N_m^+} c_{m,(n+Lq)}\, g_1(n)z^{-n}\Bigg]. \end{aligned} \tag{26}$$

By decomposing the masking filter and assuming that $(N_m^+ + 1) = 2K_dM$, with K_d analogous to the value of K in the standard CMT design, we can write

$$\begin{aligned} H_m(z) = \sum_{q=0}^{Q-1}\Bigg[&z^{-Lq}H_{b1q}(-z^{2M}) \\ &\times \sum_{j=0}^{2M-1} c_{m,(j+Lq)}\, z^{-j}E'_j(-z^{2M})\Bigg] \end{aligned} \tag{27}$$

where the polyphase decomposition of the base filter is given by

$$H_{b1q}(z) = \sum_{k=0}^{K_c-1} h_b(kQ+q)z^{-k} \tag{28}$$

for $q = 0, 1, \ldots, (Q-1)$, and the masking filter polyphase decomposition is given by

$$E'_j(z) = \sum_{k=0}^{K_d-1} g_1(2kM+j)z^{-k} \tag{29}$$

for $j = 0, 1, \ldots, (2M-1)$. Equation (27) indicates that the CMT can be implemented by using Q structures of Fig. 4, where in each one, a filter $H_{b1q}(-z^{2M})$ is placed at the input of the system, and then, the DCT-IV outputs with appropriate line permutation added to generate the M responses $H_m(z)$. Since the modulating matrices and the masking filters are the same, except for line permutations, the multiple-signal filtering structure of Fig. 7 can be used in order to simplify the overall structure.

In Fig. 7, the various input–output relationships are given by

$$Y_q(z) = z^{-1}X_q(z)E'_j(-z^2) \tag{30}$$

as desired. By rearranging the outputs after these components, it is possible to add the signals just before the premodulating matrices by dropping out some of the decimators. This leads us to the structure depicted in Fig. 8. At this point, it is worth noting that the value of K for calculating the modulating matrices and the constant c is identical to the standard CMT approach since the modulating stage remains the same. Thus, the FRM-CMT filter can be viewed as a standard CMT with prototype filter of overall order $N = LN_b + N_m^+$, where for the FRM-CMT case, we have

$$K = \frac{LN_b + N_m^+ + 1}{2M} \tag{31}$$

as seen in Fig. 8.

If both branches in the FRM design are required, this entire procedure can be applied to the lower branch, and by forcing both masking filters to have the same order $N_m^+ = N_m^- = N_m$, the responses of the two branches can be added together just before the modulating stage. In such cases, the total number of distinct coefficients, not assuming symmetry or antisymmetry of any impulse response, is given by

$$\mathcal{M} = N_b + 2N_m + 3 \tag{32}$$

and the total number of multiplications per output sample, without taking into consideration any symmetry in the subfilter coefficients, is given by

$$\mathcal{C} = (N_b + 1) + 2K_dQ + \alpha. \tag{33}$$

We also note that the value of K_c may differ for each polyphase component of the base filter. This occurs because adding more coefficients to the base filter does not misarrange the cosine modulation, as opposed to changing the masking filter length to a value other than $2K_dM$.

C. Generalized Solution for $L = 2K_aM + M/K_b$

For a more general solution, we use the results from the previous sections to derive a structure for the case where the interpolation factor is written as [4]

$$L = 2K_aM + \frac{M}{K_b} \tag{34}$$

where K_a is a non-negative integer and K_b a positive integer. In this case, (21) can be written as

$$H_m(z) = \sum_{i=0}^{N_b}\left[h_b(i)z^{-Li}\sum_{n=0}^{N_m^+} c_{m,\left[n+\left(2K_aM+\frac{M}{K_b}\right)i\right]}\, g_1(n)z^{-n}\right] \tag{35}$$

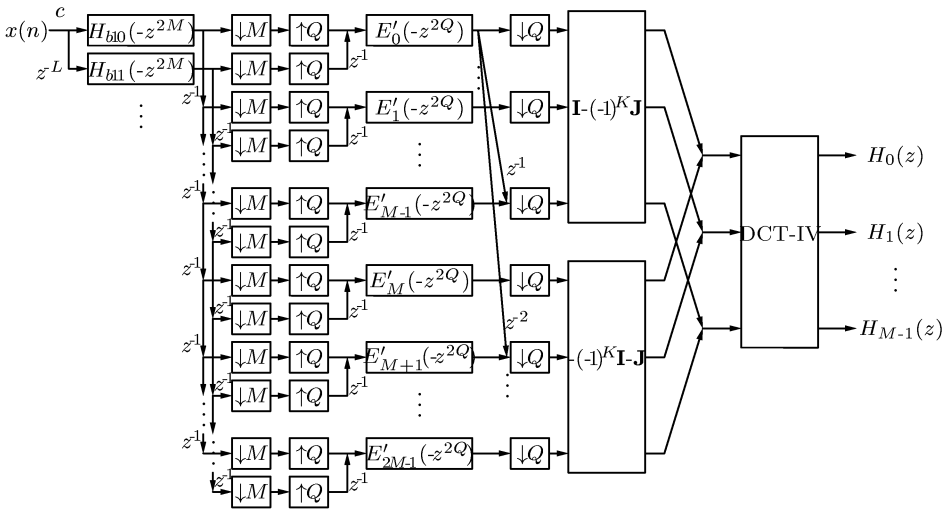

Fig. 8. CMT structure using FRM for the case when $L = M/K_b$.

and then, by using $Q = 2K_b$, $i = kQ+q$, and $(N_b+1) = QK_c$, as before, we have

$$\begin{aligned} H_m(z) &= \sum_{q=0}^{Q-1}\sum_{k=0}^{K_c-1}\Big[h_b(kQ+q)z^{-L(kQ+q)} \\ &\qquad \times \sum_{n=0}^{N_m^+} c_{m,\left[n+\left(2K_aM+\frac{M}{K_b}\right)(kQ+q)\right]} \\ &\qquad \times g_1(n)z^{-n}\Big] \\ &= \sum_{q=0}^{Q-1}\sum_{k=0}^{K_c-1}\Big[h_b(kQ+q)z^{-L(kQ+q)} \\ &\qquad \times \sum_{n=0}^{N_m^+} c_{m,\left[n+2K_aM(kQ+q)+\frac{M}{K_b}q+2kM\right]} \\ &\qquad \times g_1(n)z^{-n}\Big]. \end{aligned} \tag{36}$$

By using the relation of (11), we have

$$\begin{aligned} H_m(z) = \sum_{q=0}^{Q-1}\sum_{k=0}^{K_c-1}\Big[&h_b(kQ+q)z^{-L(kQ+q)} \\ &\times(-1)^{(k+K_akQ+K_aq)}\sum_{n=0}^{N_m^+} c_{m,\left(n+\frac{M}{K_b}q\right)}g_1(n)z^{-n}\Big] \end{aligned} \tag{37}$$

and, as Q is even, one can exploit the polyphase decomposition of $G_1(z)$, such that (37) becomes

$$\begin{aligned} H_m(z) = \sum_{q=0}^{Q-1}\sum_{k=0}^{K_c-1}\Big[&h_b(kQ+q)z^{-L(kQ+q)} \\ &\times(-1)^{(k+K_aq)}\sum_{j=0}^{2M-1} c_{m,\left(n+\frac{M}{K_b}q\right)}z^{-j}E'_j(-z^{2M})\Big]. \end{aligned} \tag{38}$$

By defining the modified polyphase components of the interpolated base filter as

$$H'_{b1q}(z) = \sum_{k=0}^{K_c-1}(-1)^{K_aq}h_b(kQ+q)z^{-k} \tag{39}$$

with $q = 0, 1, \ldots, (Q-1)$, (38) can be rewritten as

$$\begin{aligned} H_m(z) = \sum_{q=0}^{Q-1}\Big[&z^{-Lq}H'_{b1q}(-z^{LQ}) \\ &\times\sum_{j=0}^{2M-1} c_{m,\left(n+\frac{M}{K_b}q\right)}z^{-j}E'_j(-z^{2M})\Big] \end{aligned} \tag{40}$$

and we derive the structure depicted in Fig. 9, with K, as given in (31). The corresponding synthesis bank is implemented by the transposed structure of the analysis filterbank with the given base filter included.

The main difference between the structures in Figs. 8 and 9 is that in the latter, the interpolation factor of the polyphase components of the base filter is LQ instead of $2M$. If both FRM branches are present such that $N_m^+ = N_m^- = N_m$, the number of distinct coefficients of the structure depicted in Fig. 9 is given by (32), whereas its computational complexity is given by (33), as before.

The values of K_a and K_b can be chosen such that the overall FRM-CMT filter has the same order as the standard CMT design to allow a more direct comparison between the two structures. In the examples presented in the next section, we explore this design scenario. A summary of all variables of interest is given in Table I.

D. General Case with the Butterfly Structure

It can be verified that using the multiple-signal filtering structure of Figs. 7–9 is equivalent to using Q masking filters in parallel and adding their responses just before the DCT-IV operation. Thus, it is also possible to use a butterfly structure for the general case of L, as depicted in Fig. 10. In the case of $L = M$, since the butterfly-based structure requires only decimation by M, the resulting structure will not require the Q multiple-signal filtering stage. This particular but very important case is depicted in Fig. 11.

For the general case of $L = 2K_aM + (M/K_b)$, the computational complexity is reduced due to the butterfly structure that

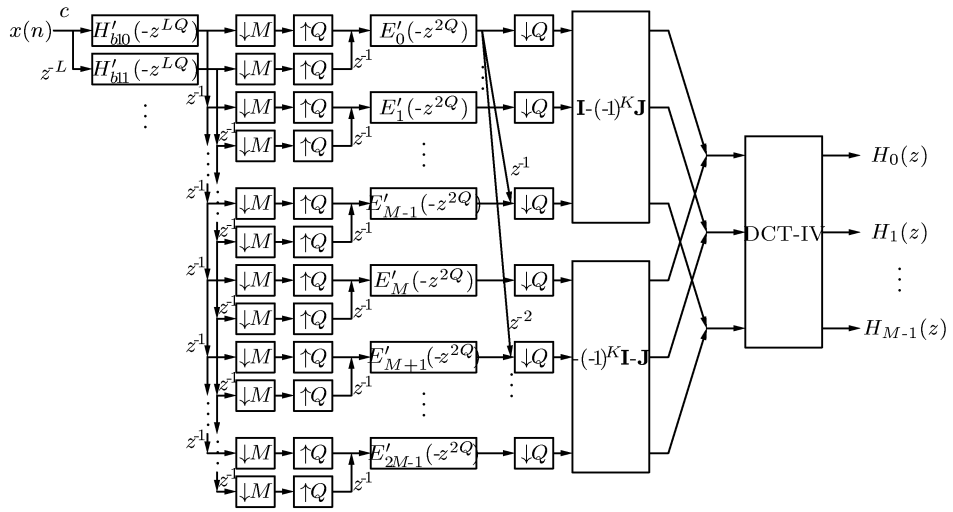

Fig. 9. CMT structure using FRM for the general case of $L = 2K_aM + M/K_b$.

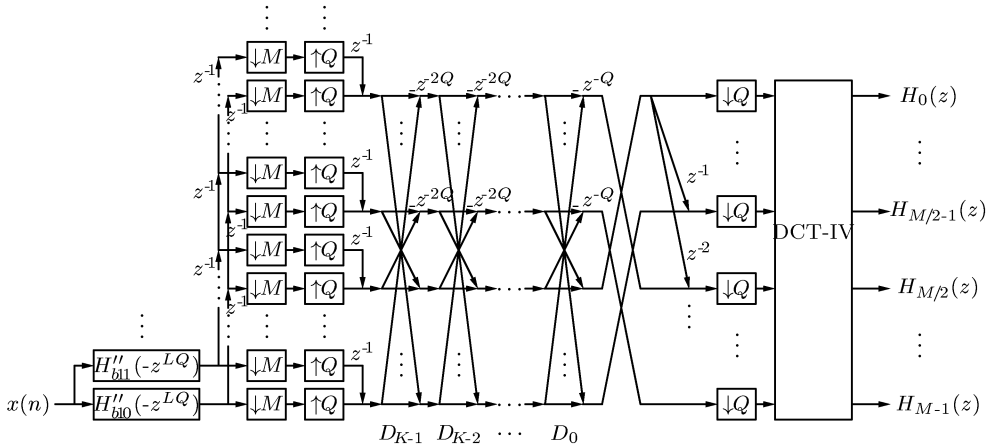

Fig. 10. Improved FRM-CMT general structure using butterflies.

TABLE I
SUMMARY OF VARIABLES OF INTEREST IN PROPOSED FRM-CMT STRUCTURE

K:	number of coefficients in each prototype-filter polyphase component.
L:	FRM interpolator factor.
M:	number of channels in the TMUX.
K_a, K_b:	factors of M in L.
K_c (K_d):	number of coefficients in each base-(masking-) filter polyphase component.
$\mathcal{M}$:	total number of distinct coefficients.
N:	order of overall prototype filter.
N_b:	order of FRM base filter.
N_m^+ (N_m^-):	order of FRM upper (lower) masking filter.
N_m:	order of masking filters when $N_m^+ = N_m^-$.
Q:	number of polyphase components for the interpolated base filter.

has fast implementation, as well as due to the fact that the interpolating factor $Q = K_b$ is half of the value for the polyphase structure case. Now, however, the modified polyphase components of the base filter are given by

$$H''_{b1q}(z) = \sum_{k=0}^{K_c-1} (-1)^{K_a(kQ+q)} h_b(kQ+q) z^{-k}. \qquad (41)$$

It is worth noting that in the butterfly-based structures given in Figs. 10 and 11, the overall PR property will depend on the base filter characteristics since the masking filter will inherently yield PR. In most practical cases, as the ones seen in the examples below, the FRM-CMT is NPR in general. There are, however, some cases where the base filter presents trivial transfer functions that result in a PR property for the entire FRM-CMT structure.

E. Multistage FRM-CMT Structure

It is possible to derive a multistage FRM-CMT structure, by using several levels of FRM design for the CMT prototype filter, to further reduce the overall computational complexity. Assuming that the lower branch is absent in the initial FRM design, the main idea is, for instance, to redesign the FRM masking filter, if the order of this filter is still too high, with other levels of the FRM approach. In this case, the original FRM-CMT L-interpolated base filter will be in cascade with

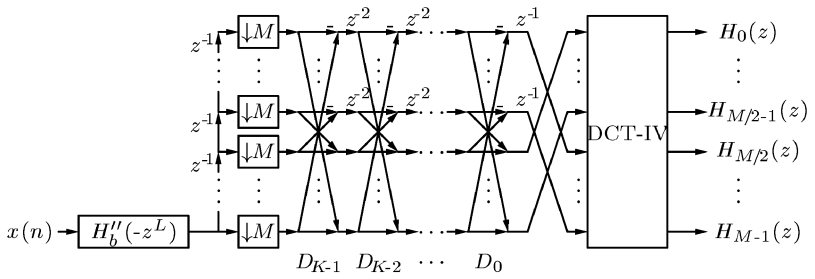

Fig. 11. Improved FRM-CMT structure using butterflies with $L = M$.

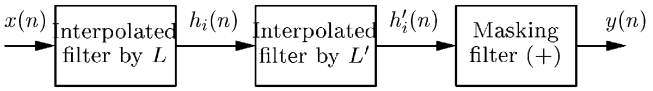

Fig. 12. FRM-CMT prototype filter using a two-stage masking-filter decomposition.

TABLE II
COMPARISON BETWEEN THE CMT DESIGNS USING OPTIMIZED DIRECT-FORM AND FRM PROTOTYPE FILTERS IN EXAMPLE 1

Method	N	$\mathcal{M}$	$\mathcal{C}-\alpha$	δ_1	δ_2	A_r	ISI	ICI
Direct	319	320	5	0.006	-74dB	73dB	-50dB	-61dB
FRM	319	69	41	0.004	-71dB	62dB	-54dB	-66dB

the second level FRM-CMT L'-interpolated base filter and corresponding masking filter, as seen in Fig. 12. For instance, if L is a multiple of L', it is then necessary to decompose the second-stage base filter by a factor of $Q' = 2M/L'$. This procedure can then be generalized to design multistage FRM-CMT systems, as seen in Example 3 below.

The corresponding computational complexity for the multistage FRM-CMT structure is given by

$$\mathcal{C}=(N_b+1)+\frac{(N_b'+1)Q'}{2M}+\frac{(N_b''+1)Q''}{2M}+\ldots+\frac{(N_m+1)Q}{2M}+\alpha \tag{42}$$

where N_b', L', and Q' are the second-stage counterparts of N_b, L, and Q, respectively, and so on.

V. NUMERICAL EXAMPLES

A. Example 1

We design a CMT with $M = 32$ channels using $\rho = 1$ and $\delta_1 \leq 0.006$. In this case, $K = 5$ should be sufficient to perform the design. Calculating the bandedge frequencies for the design of the CMT prototype filter, we obtain $\omega_p = 0.005\,469\pi$ and $\omega_s = 0.031\,25\pi$, leading to $\omega_{3\,\mathrm{dB}} \approx 0.0156\pi$. Using an optimized direct-form FIR design for the prototype filter with order $N = 2KM - 1 = 319$, we obtain the results presented in the first line of Table II [1]. By using an FRM design, we achieve the minimum number of distinct coefficients with $L = 8$, leading to $K_b = 4$ and $Q = 8$, corresponding to an overall filter order $N = 319$, as given in Table III.

TABLE III
BEST REDUCTION SCENARIO FOR THE FRM FILTER IN EXAMPLE 1

L	N_b	N_m^+	N_m^-	N	$\mathcal{M}$
8	36	31	-	319	69

As we can see from Table II, in this case, using the FRM approach leads to substantial reduction in the number of distinct coefficients, whereas the number of multiplications per output sample increased. Thus, although the filterbank implemented with the structure of Fig. 8 does not present computational complexity reduction, its design is much simpler since the number of variables (coefficients) to optimize is smaller when compared with the standard CMT design. In addition, the structure of Fig. 8 can be mapped back onto the standard structure of Figs. 4 or 5, resulting in a reduced number of operations per output sample. The FRM approach has increased the value of the minimum stopband attenuation A_r, consequently slightly increasing the value of the ICI. If we wish to reduce these values, it is possible to increase the order of the FRM filter where the number of coefficients needed may still be significantly smaller than for the direct-form implementation. Figs. 13 and 14 depict the magnitude responses of the prototype filter and the bank filters, respectively.

B. Example 2

For this second example, we designed a CMT with $M = 8$ channels, using $\rho = 0.015$ and $\delta_1 < 0.015$. Calculating the bandedge frequencies for the design of the prototype filter, we obtained $\omega_p = 0.0618\pi$ and $\omega_s = 0.0634\pi$, leading to $\omega_{3\,\mathrm{dB}} \approx 0.0625\pi$. By using the FRM approach, the best design has $L = 24$, corresponding to $K_a = K_b = 1$ and $Q = 2$, and is described in Table IV.

Table V compares the optimized direct-form and the FRM approaches for designing the CMT prototype filter. In this case, we achieved significant reductions in the number of distinct coefficients and in the overall computational complexity of the CMT system. Figs. 15 and 16 depict the magnitude responses of the prototype filter and the subfilters of the bank, respectively, in this example.

C. Example 3

In this example, a CMT with $M = 1024$ channels is designed, using $\rho = 0.1$, $A_p = 0.2$ dB, and $A_r = 50$ dB. The standard minimax design would require a filter of order $N = 88\,865$, which constitutes a nonpractical option. By using a single-stage

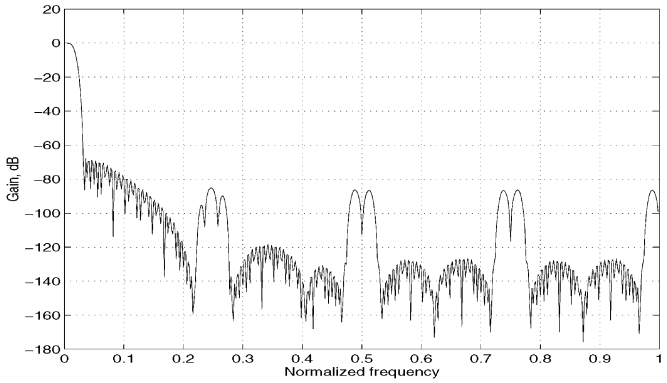

Fig. 13. Magnitude response for the FRM prototype filter in Example 1.

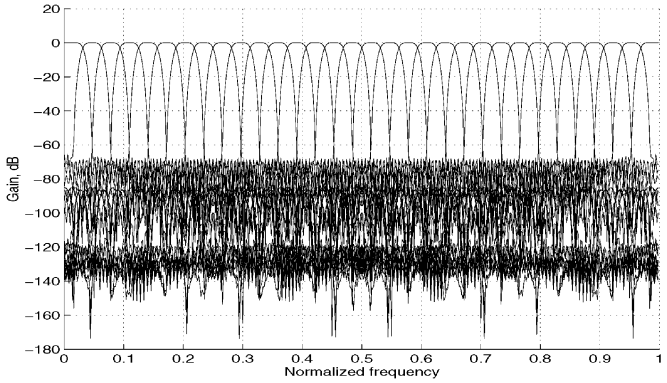

Fig. 14. Magnitude response for the CMT in Example 1.

TABLE IV
BEST REDUCTION SCENARIO FOR THE FRM FILTER IN EXAMPLE 2

L	N_b	N_m^+	N_m^-	N	$\mathcal{M}$
24	186	143	143	4607	475

TABLE V
COMPARISON BETWEEN THE CMT DESIGNS USING OPTIMIZED DIRECT-FORM AND FRM PROTOTYPE FILTERS IN EXAMPLE 2

Method	N	$\mathcal{M}$	$\mathcal{C}-\alpha$	δ_1	δ_2	A_r	ISI	ICI
Direct	4607	4608	288	0.015	-56dB	53dB	-57dB	-51dB
FRM	4607	475	223	0.009	-55dB	57dB	-50dB	-50dB

FRM-CMT, selecting $K_a = 0$ and $K_b = 4$ (thus $L = 256$ and $Q = 8$), we obtain, for the prototype filter, the results shown in the first line of Table VI. From this table, by keeping $L = 256$ and replacing the masking filter with second and third FRM stages, some computational complexity can be further reduced. However, if we change the original interpolation factor to $L = 1024$, the best reduction scenario is achieved with a three-stage FRM-CMT design, as indicated in the fourth line of Table VI.

Table VII presents the passband ripple and stopband attenuation level achieved by each multistage design described in Table VI. The prototype and filterbank responses for the first 16 channels of the three-level FRM-CMT with $L = 1024$ are shown in Fig. 17 and Fig. 18, respectively.

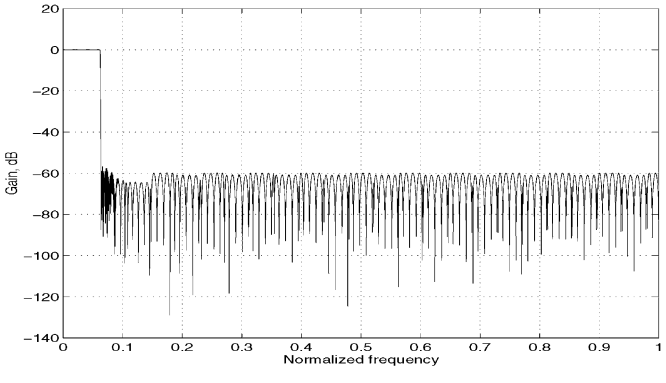

Fig. 15. Magnitude response for the FRM prototype filter in Example 2.

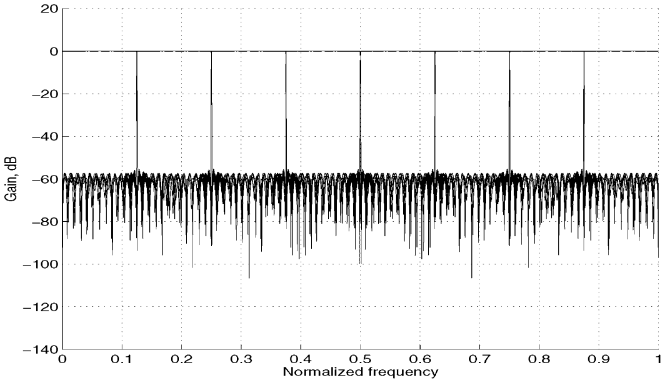

Fig. 16. Magnitude response for the CMT in Example 2.

TABLE VI
COMPARISON OF SUBFILTER CHARACTERISTICS BETWEEN MULTISTAGE FRM-CMT FILTERS IN EXAMPLE 3

Stages	L	N_b	L'	N_b'	L''	N_b''	N_m	$\mathcal{M}$	$\mathcal{C}-\alpha$
1	256	344	-	-	-	-	801	1147	348.13
2	256	344	16	66	-	-	49	462	349.39
3	256	344	16	66	4	16	17	447	353.51
3	1024	88	64	116	8	32	27	267	94.98

TABLE VII
COMPARISON OF MAGNITUDE CHARACTERISTICS BETWEEN MULTISTAGE FRM-CMT FILTERS IN EXAMPLE 3

Stages	L	A_p	A_r
1	256	0.08 dB	62 dB
2	256	0.02 dB	60 dB
3	256	0.02 dB	63 dB
3	1024	0.02 dB	64 dB

VI. CONCLUSION

In this paper, it was shown how it is feasible to design very selective transmultiplexers based on cosine modulation. By viewing the frequency-response masking (FRM) filter as a multirate system, it was possible to derive efficient filterbank realizations for a very general relationship between the number of channels M and the FRM interpolation factor L. The time delay of the resulting transmultiplex (TMUX) is not increased,

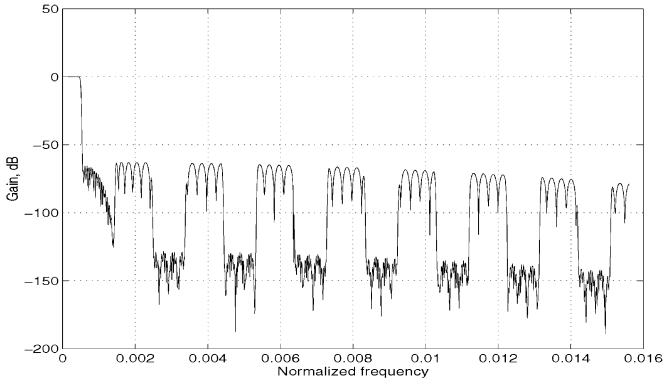

Fig. 17. Magnitude response for the three-stage FRM prototype filter with $L = 1024$ in Example 3.

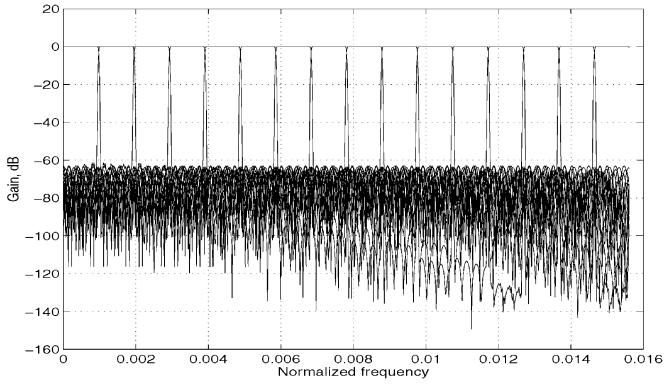

Fig. 18. Magnitude response for the three-stage CMT with $L = 1024$ in Example 3.

whereas only slight changes were observed in the other TMUX parameters of interest. The design examples confirmed that the reduction in computational complexity can be above 50%, with further reduction in the number of distinct coefficients of the prototype filter. Such a reduction allows one to design TMUX systems and filterbanks with a sharp transition band and a large number of subbands.

REFERENCES

[1] T. Saramäki, "A generalized class of cosine-modulated filter banks," in *Proc. TICSP Workshop Transforms and Filterbanks*, Tampere, Finland, June 1998, pp. 336–365.

[2] A. Viholainen, T. Saramäki, and M. Renfors, "Cosine-modulated filter bank design for VDSL modems," in *Proc. IEEE Int. Workshop Intelligent Signal Process. Commun. Syst.*, Melbourne, Australia, Nov. 1998, pp. 143–147.

[3] J. Alhava and A. Viholainen, "Implementation of nearly perfect-reconstruction cosine-modulated filter banks," in *Proc. FinSig*, Oulu, Finland, 1999, pp. 222–226.

[4] P. S. R. Diniz, L. C. R. de Barcellos, and S. L. Netto, "Design of cosine-modulated filter bank prototype filters using the frequency-response masking approach," in *Proc. IEEE Int. Conf. Acoust., Speech, Signal Process.*, vol. VI, Salt Lake City, UT, May 2001, pp. SPTM-P4.6 1–SPTM-P4.6 14.

[5] A. Viholainen, T. Saramäki, and M. Renfors, "Nearly-perfect reconstruction cosine-modulated filter bank design for VDSL modems," in *Proc. IEEE Int. Conf. Electron., Circuits Syst.*, Paphos, Greece, Sept. 1999, pp. 373–376.

[6] Y. C. Lim, "Frequency-response masking approach for the synthesis of sharp linear phase digital filters," *IEEE Trans. Circuits Syst.*, vol. CAS-33, pp. 357–364, Apr. 1986.

[7] Y. C. Lim and Y. Lian, "The optimal design of one- and two-dimensional FIR filters using the frequency response masking technique," *IEEE. Trans. Circuits Syst. II*, vol. 40, pp. 88–95, Feb. 1993.

[8] ——, "Frequency-response masking approach for digital filter design: complexity reduction via masking filter factorization," *IEEE Trans. Circuits Syst. II*, vol. 41, pp. 518–525, Aug. 1994.

[9] P. S. R. Diniz and S. L. Netto, "On WLS-Chebyshev FIR digital filters," *J. Circuits, Syst. Comput.*, vol. 9, pp. 155–168, 1999.

[10] L. C. R. de Barcellos, S. L. Netto, and P. S. R. Diniz, "Design of FIR filters combining the frequency-response masking and the WLS-Chebyshev approaches," in *Proc. IEEE Int. Symp. Circuits Syst.*, vol. II, Sydney, Australia, May 2001, pp. 613–616.

[11] H. S. Malvar, *Signal Processing With Lapped Transforms*. Boston, MA: Artech House, 1991.

[12] P. P. Vaidyanathan, *Multirate Systems and Filter Banks*. Englewood Cliffs, NJ: Prentice-Hall, 1993.

[13] P. S. R. Diniz, E. A. B. da Silva, and S. L. Netto, *Digital Signal Processing: System Analysis and Design*. Cambridge, U.K.: Cambridge Univ. Press, 2002.

[14] H. S. Malvar, "Extended lapped transforms: properties, applications, and fast algorithms," *IEEE Trans. Signal Processing*, vol. 40, pp. 2703–2714, Nov. 1992.

Paulo S. R. Diniz (F'00) was born in Niteroi, Brazil. He received the Electronics Eng. degree (cum laude) from the Federal University of Rio de Janeiro (UFRJ), Rio de Janeiro, Brazil, in 1978, the M.Sc. degree from COPPE/UFRJ in 1981, and the Ph.D. from Concordia University, Montreal, PQ, Canada, in 1984, all in electrical engineering.

Since 1979, he has been with the undergraduate Department of Electronic Engineering, UFRJ. He has also been with the graduate Program of Electrical Engineering, COPPE/UFRJ, since 1984, where he is presently a Professor. He served as Undergraduate Course Coordinator and as Chairman of the Graduate Department. He is one of the three senior researchers and coordinators of the National Excellence Center in Signal Processing

From January 1991 to July 1992, he was a visiting Research Associate with the Department of Electrical and Computer Engineering, University of Victoria, Victoria, BC, Canada. He also holds a Docent position at Helsinki University of Technology, Helsinki, Finland. From January 2002 to June 2002, he was a Melchor Chair Professor with the Department of Electrical Engineering, University of Notre Dame, Notre Dame, IN. His teaching and research interests are in analog and digital signal processing, adaptive signal processing, digital communications, wireless communications, multirate systems, stochastic processes, and electronic circuits. He has published several refereed papers in some of these areas and wrote the books *Adaptive Filtering: Algorithms and Practical Implementation* (Boston, MA; Kluwer, 2002, second ed.), and *Digital Signal Processing: System Analysis and Design* (Cambridge, U.K.: Cambridge Univ. Press, 2002) (with E. A. B. da Silva and S. L. Netto)

Dr. Diniz received the Rio de Janeiro State Scientist award from the Governor of Rio de Janeiro state. He was the Technical Program Chair of the 1995 MWSCAS held in Rio de Janeiro, Brazil. He has been on the technical committee of several international conferences including ISCAS, ICECS, EUSIPCO, and MWSCAS. He has served Vice President for region 9 of the IEEE Circuits and Systems Society and as Chairman of the DSP technical committee of the same society. He was elected Fellow of IEEE for fundamental contributions to the design and implementation of fixed and adaptive filters and electrical engineering education. He served as associate editor for the IEEE TRANSACTIONS ON CIRCUITS AND SYSTEMS II: ANALOG AND DIGITAL SIGNAL PROCESSING from 1996 to 1999, the IEEE TRANSACTIONS ON SIGNAL PROCESSING from 1999 to 2002, and the *Circuits, Systems and Signal Processing* from 1998 to 2002. He was a distinguished lecturer of the IEEE Circuits and Systems Society from 2000 to 2001. In 2004, he is serving as distinguished lecturer of the IEEE Signal Processing Society.

Luiz C. R. de Barcellos was born in Guaratinguetá, SP, Brazil. He received the B.Sc. degree from the Federal University of Rio de Janeiro (UFRJ), Rio de Janeiro, Brazil, in 1999 and the M.Sc. degree from COPPE/UFRJ in 2001, both in electrical engineering. He is currently pursuing the Ph.D. degree at COPPE/UFRJ.

Since 2002, he has been with Petrobras (Brazilian Petroleum Holding), Rio de Janeiro. His research interests are in the areas of digital signal processing, control, and communications systems.

Sergio L. Netto (M'99) was born in Rio de Janeiro, RJ, Brazil. He received the B.Sc. degree (cum laude) from the Federal University of Rio de Janeiro (UFRJ) in 1991, the M.Sc. degree from COPPE/UFRJ in 1992, and the Ph.D. degree from the University of Victoria, Victoria, BC, Canada, in 1996, all in electrical engineering.

Since 1997, he has been an associate professor with the Department of Electronics and Computer Engineering, UFRJ and, since 1998, with the Program of Electrical Engineering, COPPE/UFRJ. He is the co-author (with P. S. R. Diniz and E. A. B. da Silva) of *Digital Signal Processing: System Analysis and Design* (Cambridge, U.K., Cambridge Univ. Press, 2002). He is an associate editor for the journal *Circuits, Systems and Signal Processing*. His research interests are in the areas of digital signal processing and adaptive signal processing.

Dr. Netto is currently serving as the Vice President for Region 9 of the IEEE Circuits and Systems Society.